Journal of Applied Polymer Science

Fabrication of Polymethyl Methacrylate/Polysulfone/Nanoceramic Composites for Orthopedic Applications

Kalambettu Aravind Bhat, P. Leo Prakash, Niranjanaa Manoharan, A. Lakshmibai, Dharmalingam Sangeetha

Department of Chemistry, Anna University, Chennai 600025, Tamil Nadu, India

Correspondence to: D. Sangeetha (E-mail: sangeetha@annauniv.edu)

ABSTRACT: We report the fabrication of polymethyl methacrylate/polysulfone/nanohydroxyapatite (PMMA/PSu/nHA) and PMMA/PSu/nanotitania (PMMA/PSu/nTiO_2) composites using *N′N′*-methylene-bis-acrylamide (MBA) to crosslink PMMA and act as a blending agent. The composite was made porous by incorporating polyethylene glycol as the pore-forming agent. The blend between PMMA and PSu was confirmed using Fourier transform infrared spectroscopy and thermogravimetric analysis (TGA). The surface morphology of the composites analyzed using scanning electronic microscopy (SEM) revealed the porous structure and the wide distribution of the fillers that were found to aggregate at higher concentrations. The maximum tensile strength observed for composites was with 5% nHA (23 MPa) and 7.5% TiO_2 (30 MPa). The TGA of the composites showed better thermal stability with increase in the filler concentrations. The X-ray diffraction analysis showed that appearance of new peaks in the blend polymers indicating a strong interaction between PMMA and PSu. The surface of the composites was coated with amoxicillin and its efficiency was examined by the Zone of Inhibition test using *Streptococcus mutans*. The bioactivity of the composites was evaluated by immersing them in simulated body fluid and examining their surface for the formation of calcium-phosphate layer using SEM and EDAX. Bioactivity was found to increase with increase in filler content. The *in vitro* biocompatibility of the composites, evaluated using monkey kidney epithelial cells by MTT assay showed that the composites containing nHA showed better cell viability than the composites with nTiO_2. The study showed that the composites with nTiO_2 exhibited better strength when compared with nHA composites while the later exhibited better biocompatibility. © 2012 Wiley Periodicals, Inc. J. Appl. Polym. Sci. 000: 000–000, 2012

KEYWORDS: PMMA; PSu; nHA; nTiO_2; blend; MBA; antimicrobial activity; thermal stability; bioactivity; biocompatibility

Received 13 September 2011; accepted 28 February 2012; published online

DOI: 10.1002/app.37581

INTRODUCTION

Polymethyl methacrylate (PMMA), as a prosthetic device, has found applications in artificial lenses, dentures, limbs[1] and is also used as bone cement for the cementation of metallic and nonmetallic prostheses to bone.[2] The selection of the correct biomaterial for orthopedic prosthesis, from amongst the wide range of prosthetic materials available in the market, is dictated by some important factors such as the site of implantation, the amount of load expected to be borne by the implant, mechanical and physical properties of the implant, biocompatibility and stability of the biomaterial and the method of surgery to be employed along with the feasibility of achieving complete sterilization of the proposed implant as it would influence the development of infection at the site.[3,4] Additionally, the biomaterial could either be bioinert or bioactive and if bioactive would elicit one of the following three responses: osteoinduction, osteoconduction, or osseointegration.[5] It would be advantageous if the prosthesis, in addition to the bioactivity, possessed the ability to release drugs having a significantly local effect and thus minimize the risk of infection and inflammation. An important limiting factor in many of the polymers for application as bone substitutes is the lack of bioactivity.[2,6] Bioactivity is a desired advantage due to which direct bonding with bone can be achieved through the formation of hydroxyapatite on the surface of the polymer thus eliminating the requirement of a bone cement.[7]

When bioactivity is imparted to the PMMA, the scope of application can be extended to tissue engineering of hard tissues (bone) in situations where a nondegradable scaffold is desired. Unlike the hydrogels and smart polymers, which either swell or

degrade in aqueous medium to release the drugs incorporated within,[8] PMMA is a relatively hydrophobic polymer. One of the methods to achieve drug delivery from PMMA scaffolds is by making it porous and physically binding the desired drug to it, which will be released in the local environment. The use of porous bioactive polymer is advantageous considering the possibility of hydroxyapatite growing within the pores and thus forming an interlock with the adjacent normal bone which implies that the fixation of the polymer prosthesis would be considerably improved.[9,10] The advantage of using a polymer matrix and bioactive micro/nanofillers as biomaterials for internal bone implants is the combination of biological and mechanical properties that can be tailored for a specific medical application.[11] Mattila et al. reported that the use of PMMA based porous E-glass fiber-reinforced composite implant resulted in a mechanical inter-lock between the bone and the implant as a result of ingrowth of bone into the pores while on the other hand, fibrous tissue layer was dominant at the interface between the solid PMMA implant and bone.[12]

Sulfate group containing polymers were observed to possess good *in vitro* bioactivity.[13] Among the various sulfur group containing polymers, polysulfone (PSu) has been widely accepted for biomedical applications. It is a stable and a biocompatible polymer and has been used for hemodialysis and catheters.[14] Experiments by Spector et al.[15] demonstrated that the bone ingrowth into porous and high modulus PSu mimicked normal healing at the site of implantation.

One method to decrease the brittleness of PMMA is to blend it with another polymer having a higher elastic modulus such as PSu. However, it should be noted that PMMA and PSu are incompatible with each other apart from the fact that the tensile strength of PSu is lower than that of PMMA. Hence, blending of the two polymers would result in a polymer system with tensile strength better than that of PSu and elastic modulus better than that of PMMA.[16] Although in our previous study, we reported the successful blending of PMMA and PSu by using *N,N*-methylene-bis-acrylamide (MBA) as the blending agent,[17] in this study, we report the crosslinking of PMMA by MBA and subsequently blending it with PSu.

The use of bisacrylamides such as *N,N*-ethylene-bis-acrylamide and MBA as crosslinking agents of PMMA results in a more hydrolytically stable polymer than when dimethacrylates (2,2-bis-[4-(2-hydroxy-3 methacryloyloxypropyl)phenyl]propane (bis-GMA), triethylene glycol dimethacrylate, 1,6-bis-[2-methacryloyloxyethoxycarbonylamino]-2,4,4-trimethylhexane, and decanediol dimethacrylate (D_3MA), ethylene glycol dimethacrylate or triethylene glycol dimethacrylate are used as crosslinkers.[18,19] Additionally, the presence of amide groups provides a possibility for blend formation between incompatible polymers such as PMMA and PSu.[20] In this study, MBA was chosen as it not only crosslinks PMMA but also would result in the blending of PMMA and PSu. The proposed crosslinking of PMMA by MBA and the subsequent blend formation with PSu is illustrated in Figures 1 and 2, respectively.

The introduction of ceramic particles into the polymers results in an alteration in the chemistry along the surface which would facilitate a biochemical attachment with the bone.[21] The ceramic particles of wide interest are nanohydroxyapatite (nHA) and nanotitania ($nTiO_2$), which are both biocompatible and bioactive. Bone is a polymer composite comprised a collagen matrix with hydroxyapatite as the inorganic filler. Hence, choosing nHA will help in producing a composite which will be bioactive as well as biocompatible. Previous studies with TiO_2 as the inorganic filler revealed that apart from being bioactive, it also possessed antimicrobial activity.[22] Although many researchers have studied and reported on PMMA/HA and PMMA/TiO_2[23,24] composites, there is a scarcity in the literature reporting on PMMA/PSu/HA and PMMA/PSu/TiO_2 composites.

In this study, polymer composites of PMMA/PSu/ceramic (nHA or $nTiO_2$) were fabricated and their suitability for application as an orthopedic prosthetic device with a capability of localized drug release along with a desired level of bioactivity was evaluated. For the study, the polymer blend was made porous by incorporating a pore-forming agent, polyethylene glycol (PEG), which has a low melting temperature and is also water soluble.

MATERIALS AND METHODS

The monomer, methyl methacrylate (MMA), the polymer PSu, and the initiator benzoyl peroxide (BPO) were purchased from Sigma Aldrich while the cross linker MBA and the common solvent tetrahydrofuran were purchased from SRL, Mumbai. The inorganic fillers $nTiO_2$ (mixture of anatase and rutile form), nHA, and the pore-forming agent PEG were procured from Sigma-Aldrich.

Preparation of Crosslinked PMMA

Measured quantity of MMA was taken in a polymerization tube to which the calculated quantity of BPO and MBA was added. The solution was then heated at 70°C for 3 hr to polymerize and crosslink the MMA. The polymerization was then terminated using excess methanol and the polymer precipitated. The obtained polymer was then dried and washed repeatedly with deionized water.

Preparation of Porous PMMA/PSu/Ceramic Composite Membrane

The crosslinked PMMA was dissolved in tetrahydrofuran. PSu was then dissolved in this polymer solution by constant stirring for 8 hr. This was followed by the addition of the required quantities of the inorganic filler to form the respective groups and subgroups as detailed in Table I. To each of the above solutions, 0.25 g of PEG was added and the solutions ultrasonicated to obtain uniform dispersion of the fillers. The solution was then poured onto Petri dishes and the solvent evaporated at room temperature to obtain the composite films. These films were then heated to 50°C and washed with water to remove the PEG thus inducing pores in the composite films. The composite films were then dried and characterized.

Groups

The polymer composites were divided into two main groups viz., PMMA/PSu/nHA and PMMA/PSu/$nTiO_2$. These two groups were further subdivided into five subgroups based on the weight percentage of the filler. Groups 3 and 4 comprised only PMMA and PSu, respectively.

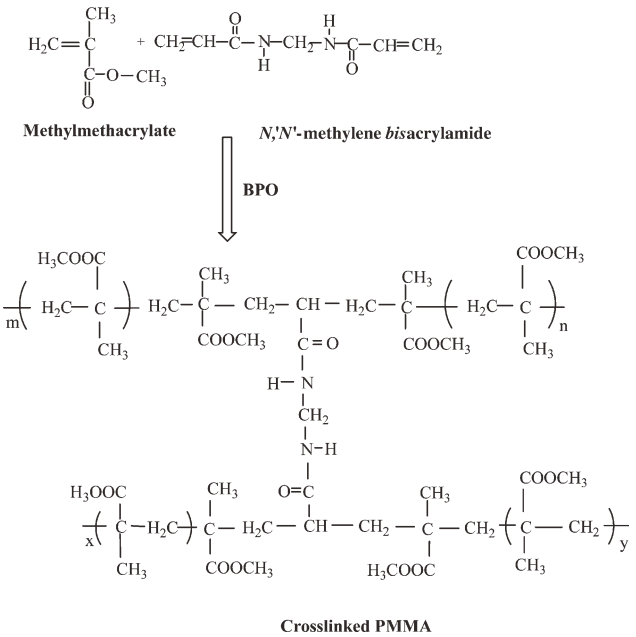

Figure 1. Crosslinking of PMMA.

Characterization

Fourier Transform Infrared Spectroscopy. The composite samples were subjected to Fourier Transform Infrared (FTIR) Spectroscopic analysis using Perkin Elmer RX I FTIR spectrophotometer to confirm the crosslinking of PMMA, to confirm the blending of PSu with the crosslinked PMMA, and to determine interaction between PMMA/PSu blend with nHA and $nTiO_2$.

X-ray Diffraction. The effect of crosslinking and addition of fillers on the crystallinity of the composites was studied by X-ray diffraction (XRD) technique using Rich Seifert X-ray diffractometer.

Thermogravimetric Analysis. The thermal analysis of the PMMA, crosslinked PMMA, PSu, and the composites was carried out using Thermogravimetric analysis (TGA) model Q50 version 20.6 build 31 systems to study the effect of crosslinking on the thermal stability of PMMA as well as to study the effect of addition of fillers on the thermal stability of the composites. The measurements were conducted by heating the samples from room temperature to 800°C at a heating rate of 10°C/min under nitrogen atmosphere.

Surface Morphology. The morphology of the composites and the distribution of the fillers in the polymer matrix were determined by Scanning electron microscopy (S-3400, Hitachi).

Evaluation of Tensile Strength. Tensile strength of the composites was analyzed by Hounsfield UTM as per ASTM-D-638. The cross head speed was set at 2 mm/min and a maximum load of 5000 N.

Estimation of Bioactivity. Bioactivity refers to the capability of the polymer membrane to induce nucleation of $Ca_3(PO_4)_2$ on its surface which then subsequently enlarges and resembles either a plaque or a coat when viewed under scanning electronic microscopy (SEM). The bioactivity property of the polymers was evaluated by analyzing the calcium phosphate layer formed on the surface of the samples after immersion in the Kokubo solution for 1 week. The samples were then retrieved, dried in an oven at 40°C for 4 hr and then examined under SEM. The samples were also subjected to EDS elemental analysis for further confirmation of the formation of the calcium phosphate layer. The simulated body fluid was prepared according to the procedure elucidated by Kokubo et al.[21]

Biocompatibility Test. Biocompatibility is the estimation of the extent of compatibility of the polymer composite with animal or human tissues. These tests are performed either *in vitro* or *in vivo*. *In vitro* tests are performed using a suitable cell culture by MTT (3-(4,5-dimethylthiazol-2-yl)-2,5-diphenyl tetrazolium bromide) method.

The biocompatibility of the composites was estimated by MTT method as described by Mossman[25] using monkey kidney

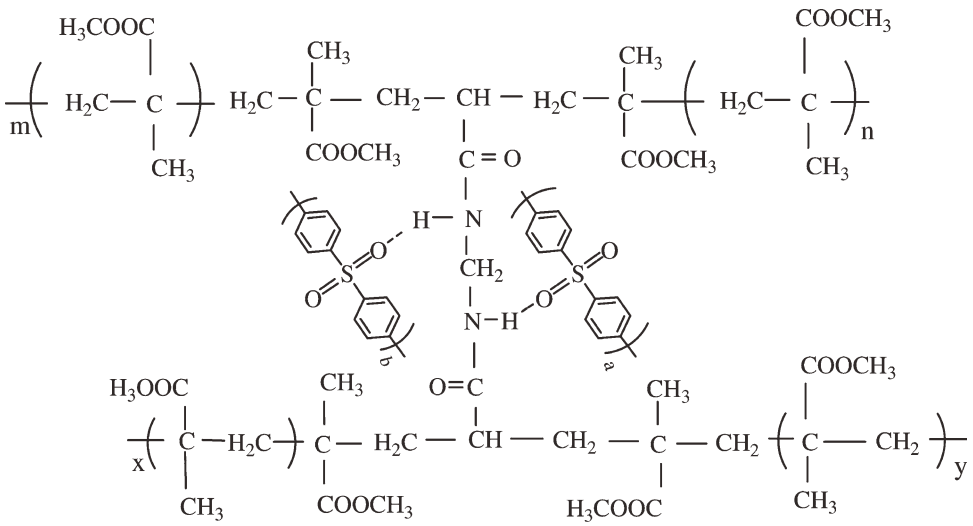

Figure 2. Blend formation between PMMA and PSu.

Applied Polymer SCIENCE

Table I. Composition of the Different Groups

S. no	Group	Group code	Composition of group
1	1	PMMA/PSu	PMMA/PSu + 0% nHA
2	1	PSH 1	PMMA/PSu + 2.5% nHA
3	1	PSH 2	PMMA/PSu + 5% nHA
4	1	PSH 3	PMMA/PSu + 7.5% nHA
5	1	PSH 4	PMMA/PSu + 10% nHA
6	2	PST 1	PMMA/PSu + 2.5% $nTiO_2$
7	2	PST 2	PMMA/PSu + 5% $nTiO_2$
8	2	PST 3	PMMA/PSu + 7.5% $nTiO_2$
9	2	PST 4	PMMA/PSu + 10% $nTiO_2$
10	3	PMMA	PMMA
11	4	PSu	PSu

epithelial cells. The percentage of viable cells gives an indication of the biocompatibility of the composite films. The experiment was performed as described later.

The composite samples were cut into suitable size and sterilized under UV radiation. They were then placed inside the wells of polystyrene culture plates (24 well). The wells were sterilized with 70% ethanol followed by UV treatment for 4 hr and neutralized with phosphate buffer (pH- 7). The wells without the membrane were the control groups for the experiment. The cells were seeded at a density of 2×10^4 cells per well and incubated at 37°C in a humidified atmosphere containing 5% CO_2. In all culture conditions, the medium was renewed every day. After 24 and 48 hr of incubation, the supernatant of each well was removed and washed with PBS. MTT diluted in serum-free medium were added to each well and the plates incubated at 37°C for 3 hr. After aspirating the MTT solution, acidified isopropanol (0.04*N* HCl in isopropanol) was added to each well and pipetted up and down to dissolve all the dark blue crystals of formazon. Finally, absorbance was measured at 630 nm using UV spectrophotometer. Each experiment was performed at least three times. The percentage cell viability was calculated by considering the values obtained for control as 100%. The obtained results were compared with those obtained for groups 3 and 4.

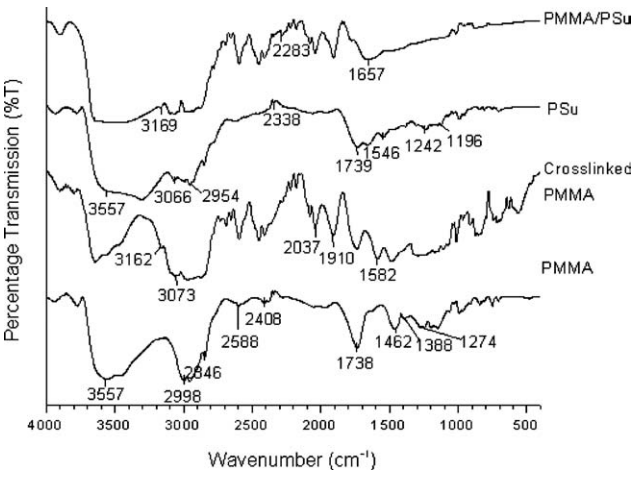

Figure 3. FTIR spectra of PMMA, crosslinked PMMA, PSu, and PMMA/PSu.

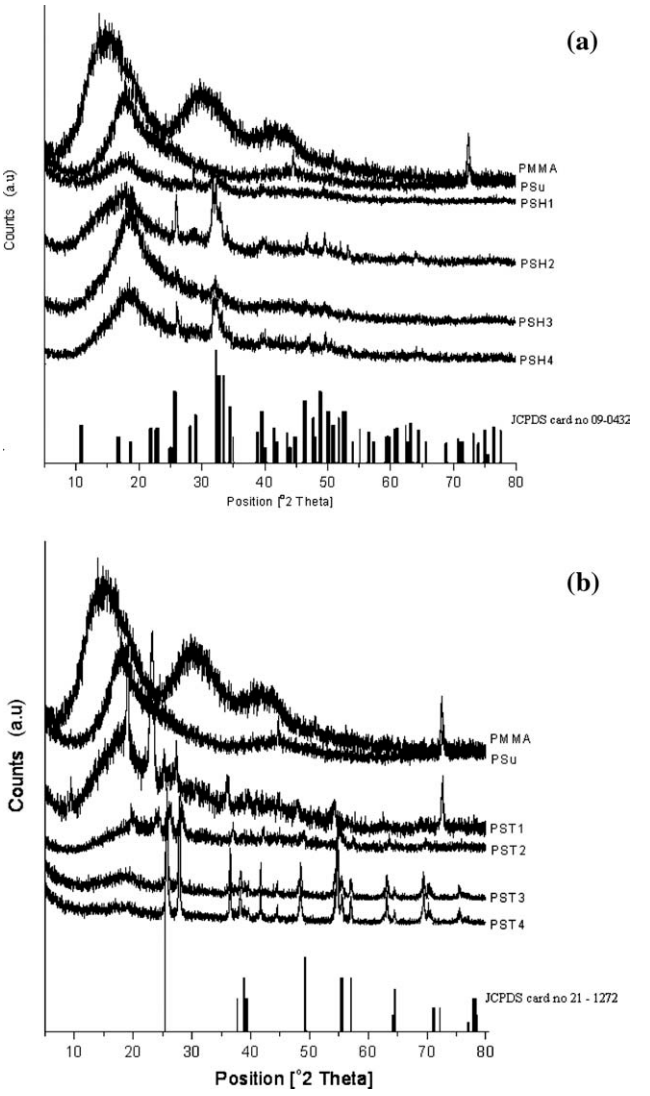

Figure 4. (a) X-ray diffractograms of PMMA/PSu/nHA and (b) PMMA/PSu/$nTiO_2$ composites.

Drug Loading and Anti-Microbial Studies. The samples were cut into 1 cm^2 dimensions and coated with amoxicillin paste. The amoxicillin paste was prepared by dissolving 2.5 g of it in 1 mL of water. This coating resulted in the physical adsorption of the drug on the surface of the composite membranes. The antimicrobial studies were carried out on *Streptococcus mutans* (*S. mutans*) cultures in agar culture medium by plate test method as detailed later.

Measured quantity of nutrient agar was dissolved in 1 L of distilled water and boiled. The Petri dishes and the agar, taken in a conical flask, were sterilized using autoclave. Subsequently, the agar was poured onto the Petri dishes under sterile conditions inside a flow chamber. Once the agar hardened, wells were created and the samples were placed within. An inoculum of *S. mutans* was then streaked over the agar medium using a sterile

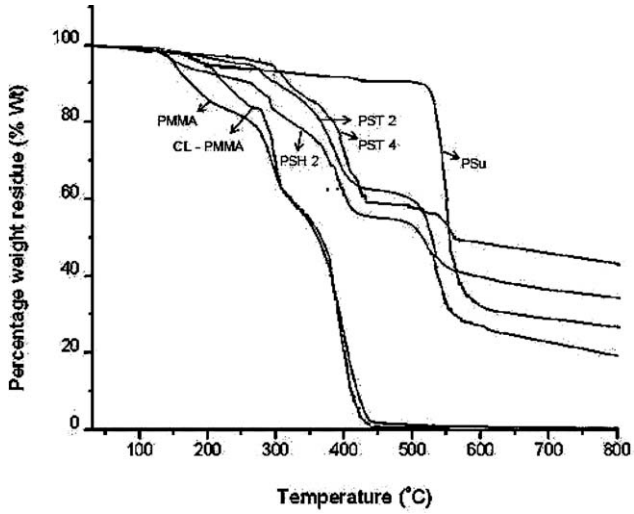

Figure 5. TGA trace of PMMA, crosslinked PMMA, PSu, and PMMA/PSu composites.

loop. The Petri dishes were labeled and incubated in an incubator for 48 hr and observed for the development of a zone of clearance around the samples. Uncoated samples acted as control.

RESULTS AND DISCUSSION

FTIR

The FTIR spectra of PMMA, crosslinked PMMA, PSu, and PMMA/PSu are shown in Figure 3. In the spectrum of PMMA, the weak peak at 1274 cm^{-1} was assigned to O—CH_3 stretching. The peak at wave number 1462 cm^{-1} was assigned to the CH_2 stretching vibrations while the peak at wave number 1738 cm^{-1} was attributed to the stretching of the C=O bond. The peak seen at 1388 cm^{-1} and the double peak at 2408 cm^{-1} represented O=C—O vibration while the broad peak at 2588 cm^{-1} is due to H—C=O stretching vibrations. The alkane CH stretching is interpreted by the occurrence of peaks at 2846 and 2998 cm^{-1}. The sharp peak observed at 3557 cm^{-1} pointed to the OH stretch, which is probably due to hydrogen bonding.

On studying the spectrum of the MBA crosslinked PMMA, it was noted that the peaks obtained were very much similar to those obtained for PMMA. However, there were some additional peaks which were attributed to the incorporation of MBA. While the peaks at 3073 and 3162 cm^{-1} were indicative of the presence of amide groups, the increase in the intensity of peaks at 1910 and 2037 cm^{-1} as compared with those of PMMA, suggested strong C=O vibrations of MBA. The sharp peak at 1582 cm^{-1} represented the bending vibrations of N—H bond. It must be noted that, because the crosslinking reaction (between PMMA and MBA) did not involve the formation of any specific bond characteristic of crosslinks, it was not possible to confirm the crosslinking of PMMA by MBA. Nevertheless, the presence of the peaks assignable to MBA suggested the presence of the crosslinking agent which otherwise would have been washed away on washing the prepared membrane with water. The additional proof of reaction between MBA and PMMA is obtained from the absence of peaks between 1640 and 1680 cm^{-1}, characteristic for C=C, indicating that crosslinking did occur between PMMA chains by MBA molecules.

In the spectrum of PSu, the peaks seen at wave numbers 1196 and 2338 cm^{-1} were due to the O=S=O symmetric stretching which is characteristic of sulfone groups. The C—H wag is observed from the medium peak at 1242 cm^{-1}. The medium peaks seen at 1546 and 1658 cm^{-1} were due to the C—C stretching and phenyl ring substitution overtones, respectively, in the PSu polymer. The S=O stretching vibrations were visualized by the peak present at 1739 cm^{-1} while the C—H stretching of the aromatic ring was evidenced by the presence of two small medium peaks at 2954 and 3066 cm^{-1}. The broad peak at 3557 cm^{-1} indicated the presence of O—H vibrations which were due to hydrogen bonding.

The spectrum of PMMA/PSu showed evidence for blend formation between the crosslinked PMMA and PSu. The peak at 2283 cm^{-1} assigned to O=S=O vibrations was found to be shifted when compared with similar peak (2338 cm^{-1}) in the spectrum of PSu. In addition, the weak hydrogen bond (proposed) formed between the amide and O=S=O of the PSu resulted in the disappearance of peak at 1196 cm^{-1}. It was also noted that transmittance peak for S=O stretching vibrations shifted to the right from 1739 cm^{-1} and now appeared at 1657 cm^{-1}. On the other hand, the peak at 3162 cm^{-1}, which was assigned to the N—H stretch from the amide group, was found to have displayed less intensity while the peak at 3073 cm^{-1} did not show any change both in intensity as well as in position. The earlier discussion validates the proposed interaction between the crosslinked PMMA and PSu via hydrogen bonding with the amide of MBA thus forming a blend of PMMA and PSu.

XRD

The X-ray diffractograms of PMMA/PSu/HA and PMMA/PSu/TiO_2 composites are shown in Figure 4(a,b), respectively. The XRD of PMMA was observed to display three broad peaks at 2 theta values of 14°, 30°, and 41°. The broad nature of the peaks and the associated vibrations was indicative of the semicrystallinity of the polymer. In the case of XRD of PSu, a single peak at 2 theta value of 18° was observed. The peak was more intense and sharper when compared with those of PMMA indicating that its crystallinity was higher than that of PMMA. The XRD pattern of PSu depicted a picture of a partially crystalline polymer.

On observing the diffractograms of the composites containing the HA filler and the peaks of HA from JCPDS card no. 09–0432 (corresponding to HA) in Figure 4(a), it was observed that the peaks for HA were present in all the composites though to a very less extent only in the case of PSH 1 which had the least concentration of HA (2.5 wt %). At the same time, it was also observed that the percentage of crystallinity of the polymer matrix appeared to decrease with increase in HA content. In other words, the amount of amorphous phase increased with increase in the HA content suggesting an interaction between the filler and the polymer matrix. The reason attributed to the exhibition of very little peaks corresponding to HA in the case of PSH 1 was that the fillers were in very less concentration and also completely wet by the polymer matrix as a result of which,

Applied Polymer SCIENCE

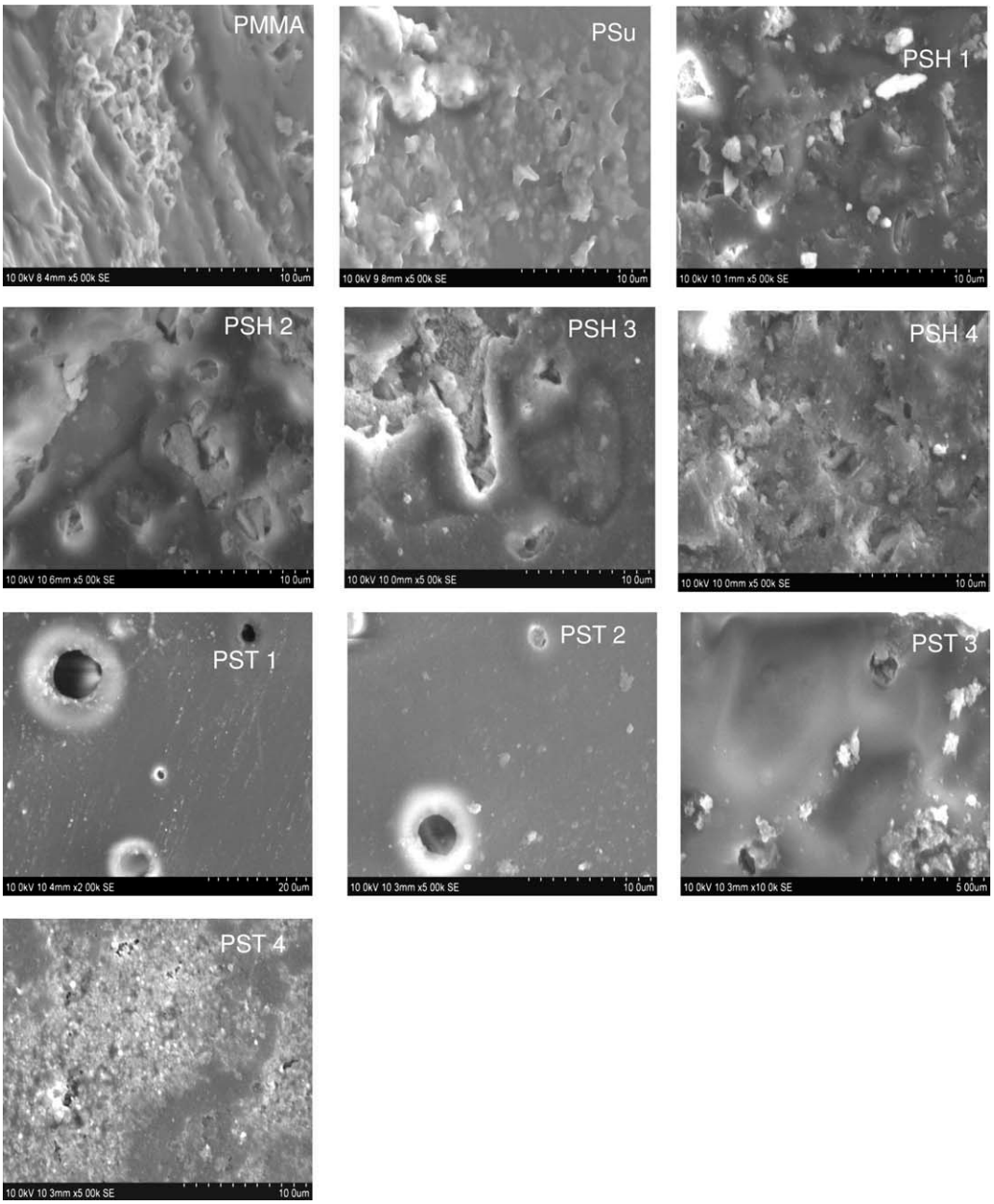

Figure 6. SEM images of PMMA, PSu, and PMMA/PSu composites.

the diffraction of the HA particles were not well resolved. On the other hand, PSH 2, 3, and 4 composites had higher percentages of HA and hence their diffractograms displayed peaks characteristic for HA.

In contrast, the diffractograms of PMMA/PSu/TiO_2 composites, shown in Figure 4(b), displayed all peaks characteristic of TiO_2 in all concentrations of TiO_2 [when compared with the diffractograms of JCPDS card no. 21-1272 corresponding to TiO_2, given in Figure 4(b)] which suggested that the TiO_2 particles were not as much wetted as seen in the case of HA. Nevertheless, as observed for PMMA/PSu/HA composites, the PMMA/PSu/TiO_2 composites also exhibited an increase in the amorphous content which was attributed again to the interaction between the filler and the matrix. From the XRD studies, it can be concluded that in both the composite types (HA and TiO_2), there was a positive interaction between the matrix resulting in a composite wherein the crystalline fillers were dispersed in a polymer matrix having a high amorphous content.

TGA

Figure 5 displays the TGA curves of PMMA, crosslinked PMMA, PSu and the composites PSH 2, PST 2, and PST 4. From the curve corresponding to PMMA, it was observed that it exhibited a three-stage degradation. This is typical of PMMA synthesized by free radical polymerization as stated by Kandare et al.,[27] in their study on PMMA composites. The first slope was associated with the loss of moisture and any adsorbed water

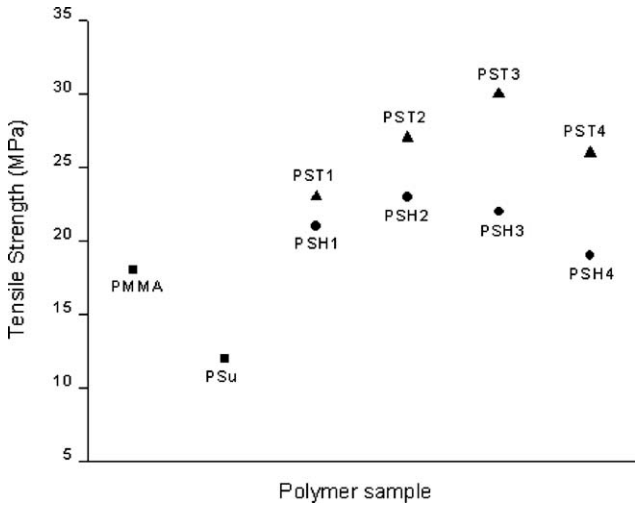

Figure 7. Tensile strength of PMMA, PSu, and PMMA/PSu composites.

molecules upto a temperature slightly higher than 100°C. The first stage of thermal degradation was initiated by scission of weak peroxide and hydroperoxide linkages as a result of the combination of monomer with O_2 during synthesis. In addition, head-to-head (H–H) linkages from termination by combination are also known to be easily broken at relatively low temperatures, leading to the production of free radicals, which would further participate in the consequential depolymerization at higher temperatures occurring through chain transfer processes. The second weight loss, largely due to the scission at the unsaturated ends, which were formed as a consequence to termination by disproportionation, involved homolytic cleavage of the C—C bond β to the vinyl group. The final weight loss was attributed to the random chain scission of the PMMA backbone.

On studying the TGA trace for the crosslinked PMMA, it was noted that it too depicted a three-stage weight loss similar to that observed in the case of PMMA. The only difference being the onset temperature for the degradation in the second stage which was increased by 20°C as compared with that of PMMA. This increase in temperature requirement could be attributed to the development of restricted chain movements of the crosslinked PMMA wherein the additional heat energy was needed to break the crosslinks due to MBA. The increase in thermal stability of PMMA on crosslinking was also reported by Shin et al.[28] who employed dispersion polymerization and crosslinked PMMA using dimethacrylates.

The TGA trace of PSu showed a two-step degradation. When in the first step, the loss in weight was associated with the loss in water molecules upto a temperature little above 100°C, further weight loss observed upto a temperature of 170°C was due to the loss of solvent molecules that were bound strongly with the polymer macromolecules during the course of reaction. It was noted that the weight loss associated with the first step (upto 170°C) was less than 5%. The second step in the weight loss, which was found to be gradual upto a temperature of little more than 500°C, was associated with degradation of the polymer backbone.

The addition of fillers resulted in an increase in thermal stability as evidenced by the TGA traces of PSH 2, PST 2, and PST 4 as compared with that of the crosslinked PMMA. The increase in the thermal stability was most probably due to an interaction between the fillers and the polymer matrix resulting in decreased mobility of the polymer chains. Additionally, the presence of the fillers would consume some of the heat and as a result more heat was required for the thermal degradation. Similar results were reported by Yang et al.[29,30] in their study with PSu and TiO_2 composites wherein, the reason attributed for the increase in stability was the presence of either a hydrogen bond or a coordination bond between TiO_2 nanoparticles and the polymer chains. This resulted in increased rigidity of the polymer chains which required more heat to break the chains while increasing the thermal stability. In this study, similar interactions were considered to have taken place between the fillers (HA and TiO_2) and the polymer matrix (PMMA and PSu) as further evidenced by the results and discussed previously under the XRD section.

On comparing the TGA traces of HA incorporated PMMA/PSu composites and TiO_2 incorporated PMMA/PSu composites, it was observed that the temperature for initiation of decomposition was much higher in the latter at comparable weight percentages of the fillers. In the Figure 6, PSH 2, PST 2, and PST 4 were alone displayed for ease in representation and comparison. It was observed that PST 2 exhibited higher thermal stability as compared with PSH 2 suggesting that in the titania-reinforced composites, the rigidity of the polymer chains was greater than that occurring in HA-reinforced composites. Evidently, this thermal stability was found to increase with increase in the filler concentration as observed by the rise in the temperature for the initiation of decomposition of PST 4 when compared with PST 2.

Surface Morphology

The surface morphology of PMMA, PSu, and PMMA/PSu composites was analyzed using SEM and the images are shown in Figure 6. The images corresponding to PMMA and PSu

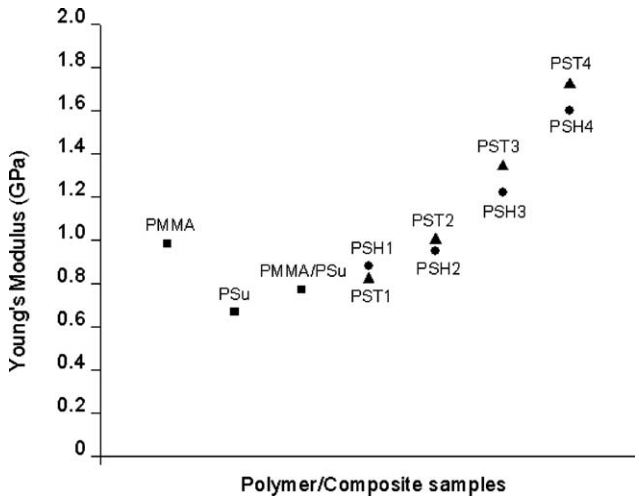

Figure 8. Elastic modulus of PMMA, PSu, and PMMA/PSu composites.

Applied Polymer SCIENCE

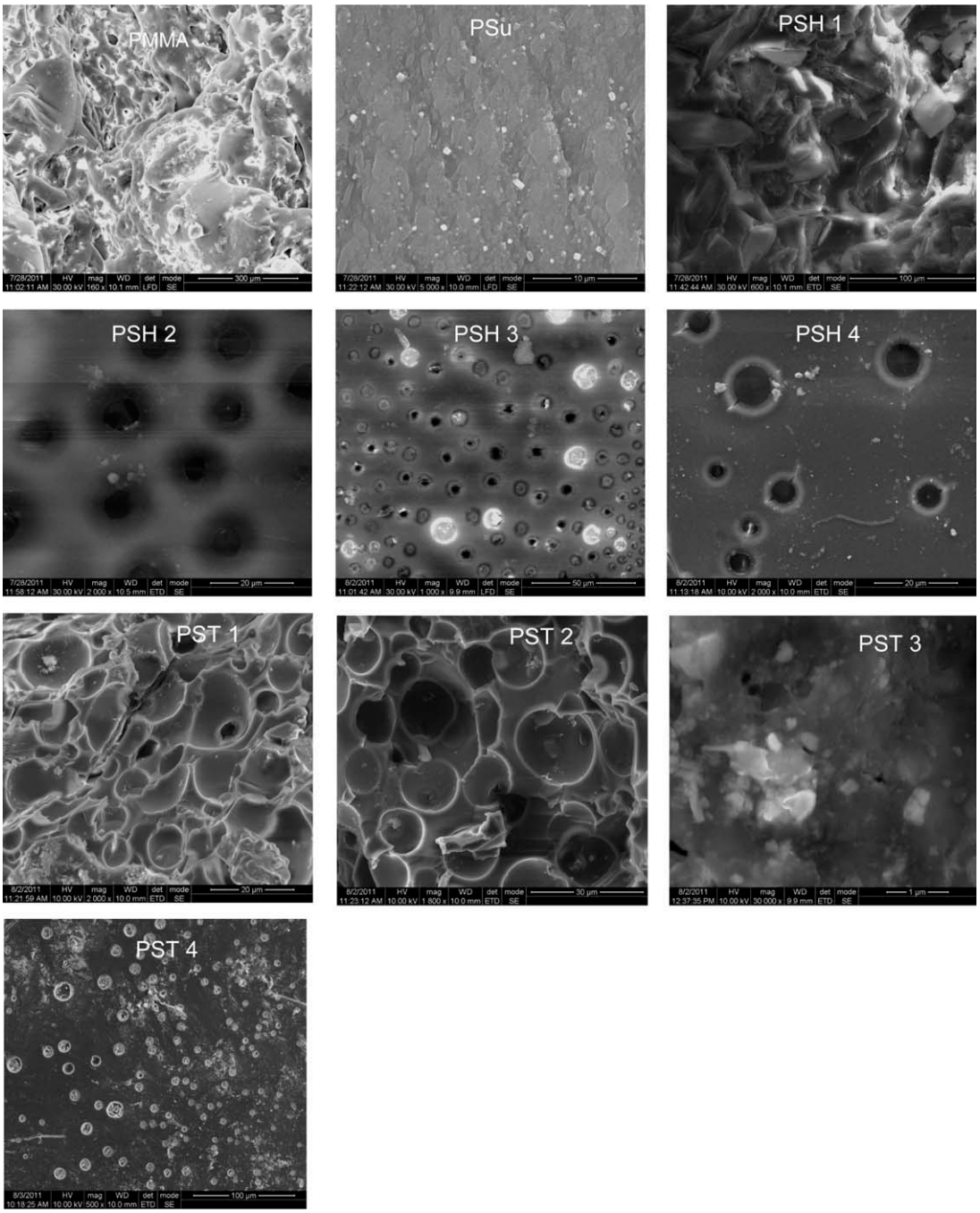

Figure 9. SEM images of PMMA, PSu, and PMMA/PSu composites subsequent to retrieval from SBF after 1 week.

displayed porous surfaces with high surface roughness. These pores were obtained by the use of PEG which was subsequently removed by washing the prepared membranes with hot water. The images corresponding to PSH 1–4 and PST 1–4 also exhibited wide spread porosities. In the case of PSH 1 and 2, the fillers were found to be quite homogenously distributed; in the case of PSH 3 and 4, the aggregation of HA particles was evident. Additionally, the pores were obscured by the presence of HA particles, which further reduced their size. In contrast, the PST 1–4 exhibited larger pores when compared with PSH composites. It was also evident that unlike in PSH composites, the TiO_2 particles did not occupy much of the pore sites. However, similar to that observed for PSH composites, PST 3 and 4 exhibited agglomeration of TiO_2, resulting in their nonhomogenous distribution in the matrix. This observation was similar to the surface morphology analysis reported by Chatterjee[31] on PMMA/nTiO_2 composites.

Evaluation of Tensile Strength

The results of the tensile strength analysis of the composites are given in Figure 7. From the figure, it was evident that PSu exhibited lesser tensile strength (13 MPa) than PMMA (18

Table II. EDS Analysis of PMMA, PSu, and PMMA/PSu Composites

Sample	Calcium (wt %)	Phosphate (wt %)
PMMA	0.16	0.10
PSu	0.24	0.18
PSH 1	2.74	3.74
PSH 2	4.26	3. 53
PSH 3	5.67	5.18
PSH 4	7.32	6.91
PST 1	2.86	1.46
PST 2	4.51	2.09
PST 3	5.18	3.34
PST 4	9.70	3.85

MPa). PMMA was stronger and brittle when compared with PSu. The addition of PSu was expected to increase the plasticity while the addition of the fillers was expected to increase the tensile strength and offset the negative effect of the PSu on the tensile strength of the resulting composites. The negative effect of PSu on the blend was evident by observing the decreased tensile strength of the blend polymer (PMMA/PSu) as against that of PMMA. In general, it was noted that PST composites exhibited greater strength than PSH composites. The reason for the higher strength of PST composites could probably be their better filler distribution and interaction with the polymer matrix.

On comparing the PSH 1–4, PSH 2, which contained 2.5 wt % of HA, exhibited maximum tensile strength. Further increase in concentration resulted in a decrease in the tensile strength. This was attributed to the problem of agglomeration and non uniform distribution of the filler particles at higher concentrations (discussed under surface morphology section), as a result of which areas susceptible to fracture were created. In the PST group, PST 3, which had 7.5 wt % of TiO_2, exhibited the highest tensile strength (30 MPa), which was about twice of that observed for PMMA. Though PST 3 also exhibited agglomeration of the filler particles, it appeared that its interaction with the polymer macromolecules resulted in an increase in their rigidity with a consequent increase in the tensile strength. However, further increase in the filler content was detrimental to the strength of the composite. Nevertheless, from the values of modulus of elasticity (Figure 8), it was evident that the blend polymer (PMA/PSu) exhibited lower modulus than PMMA which was attributed to influence of PMMA and PSu on each other. From Figure 8, it is also evident that with increase in the filler content the modulus of elasticity also increased. When this observation is correlated with the results of the tensile strength, it can be inferred that the addition of fillers not only increases the tensile strength but also imparts stiffness to the composite. At the same time, comparing the results of PSH and PST samples, it was noted that PST samples produced higher modulus values. This was attributed to the interaction between the $nTiO_2$ fillers and the polymer matrix, as explained by Chatterjee,[31] resulting in decreased movement of the polymer chains.

While it is acknowledged that the use of coupling agents such as 3-(trimethoxysilyl) propyl methacrylate[23] and 2-hydroxy ethyl methacrylate[24] would result in enhanced interaction between the inorganic fillers and the polymer matrix, in this study no such coupling agents were employed and the results obtained were due to the physical interaction of the fillers with the polymer matrix. It can thus be expected that the composites would display better tensile properties when these coupling agents are employed. Nonetheless, Chatterjee[31] showed that there was a chemical interaction between TiO_2 and PMMA either in the form of H-bond between carbonyl group and surface hydroxyl group of TiO_2 or the binding of TiO_2 with two oxygen atoms of COOR by a bidentate coordination to Ti^{4+} cation.

The tensile properties of the composite films prepared in this study was much inferior to those observed by Tham et al.,[23] who reported values of $\sim$ 50 MPa for PMMA and $\sim$ 35 MPa for PMMA/HA (5 wt %) composites. One major reason attributed to the difference in tensile strength was the method of fabrication of the composite wherein Tham et al employed the traditional dental laboratory method of fabricating dentures using heat to initiate polymerization and employing prepolymerized PMMA powder as an additional reinforcement. However, it was found that the tensile values of the composite membranes (both PSH and PST) reported in this study were higher than those reported in our earlier study wherein PMMA was not crosslinked but only blended with PSu using MBA and 0.25 wt % β-Tricalcium phosphate was employed as the filler.[17] The higher tensile strength observed in this study could be the result of two factors—crosslinking of PMMA and incorporation of higher amounts of filler. It should also be noted that the samples tested in this study were porous in nature unlike the solid samples reported in the literature.[17,23,24,28] In comparison, studies by Hong et al.[32] showed that the addition of silica fillers along with a coupling agent to PMMA matrix resulted in an increase in tensile strength by 96% while the elastic modulus was increased by 193%. From the earlier discussion, it is evident that the incorporation of PSu resulted in a decrease in the elastic modulus of the composite implying that PMMA/PSu/ceramic composites would withstand stress better than PMMA/Ceramic composites.

Table III. Percentage Cell Viability of PMMA, PSu, and PMMA/PSu Composites

Sample	Percentage of viable cells
PMMA	65
PSu	85
PMMA/PSu	71
PSH 1	74
PSH 2	81
PSH 3	80
PSH 4	84
PST 1	73
PST 2	75
PST 3	74
PST 4	74

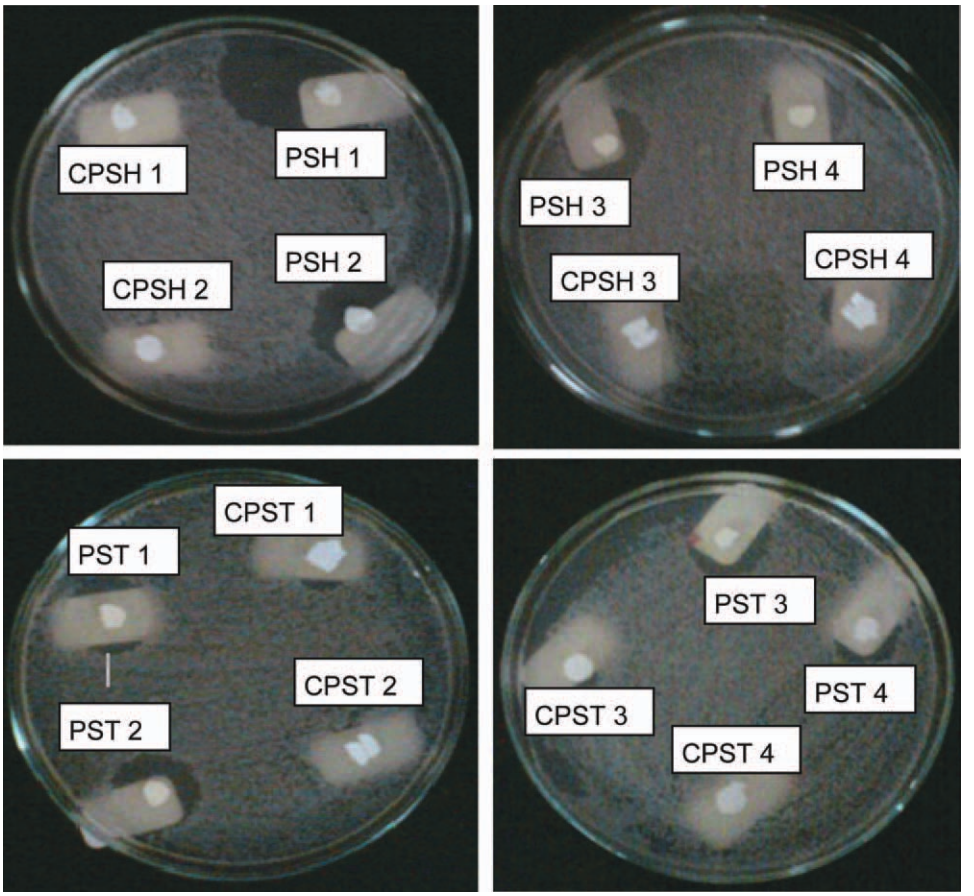

Figure 10. Photograph of zone of inhibition test. The prefix C before the sample code indicates the uncoated sample which functioned as the negative control. [Color figure can be viewed in the online issue, which is available at wileyonlinelibrary.com.]

Evaluation of Bioactivity

The SEM images of the samples subjected to immersion in SBF are shown in Figure 9. In the SEM images of PMMA and PSu, negligible bioactivity was observed. In comparison, PSH 1 exhibited very good nucleation and deposition of calcium phosphate crystals resembling hydroxyapatite followed by PSH 3 and 4. The greater amount of mineral deposition on the surface of PSH 1 is believed to be due to the homogenous distribution and good wetting of the HA fillers by the polymer matrix. Similar *in vitro* studies by Arcos et al.[33] and Dalby et al.[34] showed that the incorporation of HA into PMMA not only enhanced the growth of apatite-like layer on the surface of the composite but also resulted in an increased proliferation of human osteoblast-like cells associated with a higher alkaline phosphatase activity.

In the PST composites, it was observed that PST 3 and 4 showed evidence of higher calcium phosphate deposition than PST 1 and 2 despite the filler particles being agglomerated. The passive dissolution of TiO_2 was responsible for the hydrolysis of titania resulting in the formation of OH^- and $Ti(OH)_n^{(4-n)+35}$ The OH^- ions get adsorbed on the oxide surface forming Ti–OH groups, and subsequently promote the nucleation of Ca–PO_4 on the surface of the composite. In this context, it is appropriate to bring in the observations of Uchida et al.[36] who in their study found that while the titania gels, with an amorphous structure, failed to induce apatite formation on their surfaces in the simulated body fluid, gels with an anatase or rutile structure induced apatite formation. The crystalline planar arrangement in the anatase structure was thought to facilitate epitaxy of the apatite crystals on the surface. In this study, because the $nTiO_2$ used was a mixture of anatase and rutile crystal structures, the bioactivity observed is in accordance with the results of Uchida et al. It is also of interest to note that in the *in vivo* experiments of Goto et al.[37] maximum osteoconduction was seen in PMMA/TiO_2 composites having 60 wt % of silanized filler.

The bioactivity of the composites was further evaluated using EDS analysis. The results of the EDS test are given in Table II. It was observed that while PMMA and PSu showed very little evidence of bioactivity, the quantity of Ca and PO_4 were found to increase with increase in the hydroxyapatite concentration in PSH composites.

However, these results need to be cautiously taken because these composites already contain Ca–PO_4 in the hydroxyapatite form which would also be calculated along with the nucleation/deposition of new Ca–PO_4 layer. On the other hand, the PST composites showed much greater nucleation/deposition of Ca–PO_4 than their PSH counterparts as evidenced by the values in Table II. The amount of Ca–PO_4 nucleated/deposited on the PST

composites was found to increase with increase in the filler concentration.

Biocompatibility Test

The results of the percentage cell viability are tabulated in Table III. It was evident that PMMA exhibited some amount of toxicity to the epithelial cells while PSu was very much biocompatible. Interestingly, the cytotoxicity was found to decrease in the case of PMMA/PSu blend polymer. The higher cytotoxicity seen with PMMA could be due to the presence of some unreacted monomer or due to BPO. In the case of the blend, this effect was offset by the presence of amide groups. Additionally, the wt% of PMMA in the case of blend was only 50%. The PSH composites exhibited higher cell viabilities for higher HA wt%. Zhang et al.[38] observed similar findings wherein, the toxicity to gingival fibroblasts was found to decrease with increase in the concentration of HA filler in the PMMA matrix. In the case of PST composites, the percentage of cell viability ranged between 73 and 75, which was close to that observed for PMMA/PSu blend thus indicating that the presence of TiO_2 did not influence the biocompatibility as much as nHA did.

Antimicrobial Study

The images of the zone of clearance obtained in the plate test are depicted in Figure 10. From the figure, it was observed that while none of the control samples developed any zone of clearance, all the drug loaded samples were surrounded by a minimum of 1.5-cm diameter of zone of clearance. This indicated that this method of coating the antibiotic over the surface of the proposed prosthetic material is effective in warding out potential infections at the site of implantation thus eliminating the need for systemic antibiotic regimen following implantation of the prosthetic device. In a related study, Arcos et al. showed that the bioglass/PMMA composite released the drug gentamycin at high levels during the first few hours in SBF after which the release tapered down but was sufficient enough to act as a maintenance dose.[33] It should however be noted that, while in this study, the drug amoxicillin was coated over the surface of the composite, Arcos et al. incorporated the drug gentamycin within the composite using a different methodology.

CONCLUSION

PMMA was crosslinked by a novel method using MBA in a process where polymerization as well as crosslinking took place simultaneously. Following this, PSu was successfully blended with PMMA as evidenced by FTIR, TGA, and XRD analysis. The characterization studies of the composites revealed that the physical and thermal properties were influenced by both type (either nHA or $nTiO_2$) and quantity of filler incorporated into it. PST composites exhibited better tensile strength and bioactivity when compared with PSH composites. From the tensile test, it could be inferred that PSu played a role in reducing the stiffness of PMMA which would potentially enhance the function of the composite when used as an implant, especially as a bone defect filling biomaterial. In particular, among all the composites, highest bioactivity was witnessed for PST 4 having 10 wt % TiO_2. The porous morphology was also found to be influenced by the filler type and the titania containing composites showed greater pore size. The presence of MBA was believed to enhance the biocompatibility of the polymer matrix as evidenced by the increase in cell viability percentage of PMMA/PSu polymer and composites. When the overall properties of all the fabricated composites were compared, it can be concluded that PST 3 having 7.5 wt % of TiO_2 gave the optimum performance. The results of the plate test would suggest that when such composites, intended to be used as bone filling membranes at the site of bone defects, are coated with a broad spectrum antibiotic, it would eliminate the need for systemic antibiotic regimen by facilitating localized drug delivery and thus preventing the onset of infection at the site of implantation. Additionally, anti-inflammatory agents could also be coated which would reduce any inflammation that would occur at the site.

ACKNOWLEDGMENTS

The authors would like to thank CTDT, Anna University, Chennai and ICMR, New Delhi for funding the study (ICMR Letter No. 5/20/5(Bio)/09-NCD-1). The authors acknowledge the help rendered by King's Institute, Chennai, in carrying out the biocompatibility testing.

REFERENCES

1. Frazer, R. Q.; Byron, R. T.; Osborne, P. B.; West, K. P. *J. Long Term Effects Med. Implants* **2005,** *15*, 629.
2. Park, J. B. *Ann. Biomed. Eng.* **1992,** *20*, 583.
3. Vuyk, H. D.; Adamson, P. A. *Clin. Otolaryngol.* **1998,** *23*, 209.
4. Darouiche, R. O. *N. Engl. J. Med.* **2004,** *350*, 1422.
5. Albrektsson, T.; Johansson, C. *Eur. Spine J.* **2001,** *10*, S96.
6. Tsukeoka, T.; Suzuki, M.; Ohtsuki, C.; Sugino, A.; Tsuneizumi, Y.; Miyagi, J.; Kuramoto, K.; Moriya, H. *Biomaterials* **2006,** *27*, 3897.
7. Harper, E. J. *J. Eng. Med.* **1998,** *212*, 113.
8. Qiu, Y.; Park, K. *Adv. Drug Delivery Rev.* **2001,** *53*, 321.
9. Kokubo, T. *Mater. Sci. Eng. C* **2005,** *25*, 97.
10. Clark, P. A.; Moioli, E. K.; Sumner, D. R.; Mao, J. J. *FASEB J.* **2008,** *22*, 1684.
11. Pielichowska, K.; Blazewicz, S. *Adv. Polym. Sci.* **2010,** *232*, 97.
12. Mattila, R. H.; Laurila, P.; Rekola, J.; Gunn, J.; Lassila, L. V. J.; Mantyla, T.; Aho, A. J.; Vallittu, P. K. *Acta Biomater.* **2009,** *5*, 1639.
13. Arias, J. L.; Carrillo, A. N.; Arias, J. I.; Escobar, C.; Bodero, M.; David, M.; Fernandez, M. S. *J. Mater. Chem.* **2004,** *14*, 2154.
14. Nakashima, A.; Ogata, S.; Doi, S.; Yamahira, M.; Naraki, S.; Takasugi, N.; Ohmoto, T.; Ito, T.; Masaki, T.; Yorioka, N. *Clin. Exp. Nephrol.* **2006,** *10*, 210.
15. Spector, M.; Michno, M. J.; Smarook, W. H.; Kwiatkowski, G. T. *J. Biomed. Mater. Res. Part A* **1978,** *12*, 665.
16. http://www.ides.com/info/generics/3/C/T/Acrylic-Acrylic-Properties-Processing
17. Bhat, K. A.; Rajangam, P.; Dharmalingam, S. *J. Mater. Sci.* DOI 10.1007/s10853-011-5892-y

18. Moszner, N.; Fischer, U. K.; Angermann, J.; Rheinberger, V. *Dental Mater.* **2006,** *22*, 1157.
19. Kratz, K.; Lapp, A.; Eimer, W.; Hellweg, T. *Colloids Surf. A: Physicochem. Eng. Aspects* **2002,** *197*, 55.
20. Deimede, V. A.; Fragou, K. V.; Koulouri, E. G.; Kallitsis, J. K.; Voyiatzis, G. A. *Polymer* **2000,** *41*, 9095.
21. Li, P.; Ohtsuki, C.; Kokubo, T.; Nakanishi, K.; Soga, N.; Nakamura, T.; Yamamuro, T. *J. Mater. Sci. Mater. Med.* **1993,** *4*, 127.
22. Vinodh, R.; Bhat, K. A.; Sangeetha, D. *J. Polym. Res.* **2011,** *18*, 1469.
23. Tham, W. L.; Chow, W. S.; Mohd Ishak, Z. A. *J. Appl. Polym. Sci.* **2010,** *118*, 218.
24. Yeh, J.; Weng, C.; Huang, K.; Huang, H.; Yu, Y.; Yin, C. *J. Appl. Polym. Sci.* **2004,** *94*, 400.
25. Mosmann, T. *J. Immunol. Methods* **1983,** *65*, 55.
26. Hermanson, N. J. *Med. Plastics Biomater.* **2008** Available at: http://www.mddionline.com/article/syndiotactic-polystyrene-new-polymer-high-performance-medical-applications
27. Kandare, E.; Deng, H.; Wang, D.; Hossenlopp, J. *Polym. Adv. Technol.* **2006,** *17*, 4.
28. Shin, J.; Bae, W.; Kim, H. *Colloid. Polym. Sci.* **2010,** *288*, 271.
29. Yang, Y.; Wang, P.; Zheng, Q. *J. Polym. Sci. Part B: Polym. Phys.* **2006,** *44*, 879.
30. Yang, Y.; Wang, P. *Polymer* **2006,** *47*, 2683.
31. Chatterjee, A. *J. Appl. Polym. Sci.* **2010,** *116*, 3396.
32. Hong, R. Y.; Fu, H. P.; Zhang, Y. J.; Liu, L.; Wang, J.; Li, H. Z.; Zheng, Y. *J. Appl. Polym. Sci.* **2007,** *105*, 2176.
33. Arcos, D.; Ragel, C. V.; Vallet-Regi, M. *Biomaterials* **2001,** *22*, 701.
34. Dalby, M. J.; Di Silvio, L.; Harper, E. J.; Bonfield, W. *J. Mater. Sci.: Mater. Med.* **1999,** *10*, 793.
35. Healy, K. E.; Ducheyne, P. In Medical Applications of Titanium and its Alloys: the Material and Biological Issues, ASTM STP 1272; Brown, S. A., Lemons, J. E., ed.; American Society for Testing and Materials: Philadelphia, **1996.**
36. Uchida, M.; Kim, H.; Kokubo, T.; Fujibayashi, S.; Nakamura, T. *J. Biomed. Mater. Res. Part A.* **2003,** *64A*, 164.
37. Goto, K.; Tamura, J.; Shinzato, S.; Fujibayashi, S.; Hashimoto, M.; Kawashita, M.; Kokubo, T.; Nakamura, T. *Biomaterials* **2005,** *26*, 6496.
38. Zhang, J.; Liao, J.; Mo, A.; Li, Y.; Li, J.; Wang, X. *Appl. Surf. Sci.* **2008,** *255*, 328.